Scanning Probe Microscopy

DOI: 10.1002/anie.200704731

Subnanometer-Resolved Patterning of Bicomponent Self-Assembled Monolayers on Au(111)**

Giuseppina Pace, Anne Petitjean, Marie-Noëlle Lalloz-Vogel, Jack Harrowfield, Jean-Marie Lehn, and Paolo Samorì**

The controlled spatial confinement of individual functional nano-objects on surfaces is of paramount importance for studying single-molecule properties, such as reactivity and kinetics,[1] thus paving the way for new applications in the fields of (bio)chemical sensors and molecular electronics, and ultimately, for the miniaturization of electronic devices. Numerous molecular switches and motors have been proposed.[2] However, although the dynamic properties of such molecular devices have been thoroughly characterized in solution, very little has been done to exploit their characteristics for the development of electronic (nano)devices operating on surfaces.[3,4] The major restrictions are represented by constraints introduced by the solid surface, for example, the molecule–substrate interactions, the steric hindrance caused by dense packing at the surfaces (thus reducing the molecular conformational freedom), the instability and uncertainty in the location of the binding, and so on. All these factors drastically affect the well-established solution properties and hamper the applicability of these molecules in functional molecular devices.

Of particular importance—as a first step—is the building up, with nanoscale precision, of highly ordered multicomponent arrays of functional units on solid substrates to make the active functional groups easily accessible. This ordered spatial confinement of single active molecules permits an ultimate control of the single-molecule properties when an external stimulus is applied and, on the long term, it should make it possible to shrink the size of electronic memory bits to the limit of a single molecule.

[*] Dr. G. Pace, Dr. A. Petitjean, M.-N. Lalloz-Vogel, Prof. J. Harrowfield, Prof. J.-M. Lehn, Prof. P. Samorì
ISIS/CNRS UMR 7006—Université Louis Pasteur
8 allée Gaspard Monge, 67000 Strasbourg (France)
E-mail: lehn@isis.u-strasbg.fr
Prof. P. Samorì
ISOF-CNR, via Gobetti 101
40129 Bologna (Italy)
E-mail: samori@isis-ulp.org
Dr. A. Petitjean
Queen's University, 90 Bader Lane
Kingston, ON, K7L 3N6 (Canada)

[**] This work was supported by the EU through the projects Marie Curie EST—SUPER (MEST-CT-2004-008128), RTN Marie Curie RTNs PRAIRIES (MRTN-CT-2006-035810), and THREADMILL (MRTN-CT-2006-036040), the ERA-Chemistry project SurConFold, the ESF-SONS2-SUPRAMATES project, and the Regione Emilia-Romagna PRIITT Nanofaber Net-Lab.

Supporting information for this article is available on the WWW under http://www.angewandte.org or from the author.

Among the different methodologies proposed for the assembly of functional molecules on solid substrates, the chemisorption of self-assembled monolayers (SAMs) on gold is the most widely studied and characterized one. The easy preparation and high stability of the monolayers make them an ideal system for further improving the control over the assembly of active molecules on gold.[5]

In spite of the good control that has been achieved on the molecular binding and packing of monocomponent SAMs (of, for example, alkanethiols or arenethiols) on Au(111),[6] it is still very difficult to prepare mixed SAMs in which a single active component can be easily addressed.

Many efforts have been devoted to the isolation of single active molecules as guests in a hosting SAM.[1,7] Unfortunately, mixing two thiolated compounds on a metallic substrate leads either to phase segregation[8] of the two components in separate single-component domains[9–11] or to the insertion of the guest molecules at defect sites of the hosting molecular matrix.[5c,9,12–14] The latter case allows for the spatial confinement of active molecules, but their location at defect sites reflects the poor stability of the molecule–substrate bond, which leads to great uncertainty in the measured molecular properties. In fact, single molecules or small molecular clusters chemisorbed at defect sites can easily diffuse, desorb, and re-adsorb, and they are more subject to conformational fluctuations because of the lack of lateral packing.

Folkers et al. used the Bragg–Williams approach to describe the behavior of SAMs formed from multicomponent solutions.[13] Their model predicted the possibility of obtaining fully miscible and crystalline multicomponent SAMs by designing molecules with favorable heteromolecular interactions and the tendency to form metastable intermixed crystalline domains. However, crystalline multicomponent domains, within chemisorbed SAMs, have not been observed so far.

We devise a new and general approach to tailor multicomponent crystalline SAMs by using the basic principles of supramolecular chemistry,[15] thereby achieving control over the spatial confinement of functional nano-objects on surfaces (with subnanometer resolution). Submolecularly resolved STM imaging provides direct evidence of the formation of such crystalline mixed SAMs.

To avoid phase segregation and foster a complete miscibility between two molecular components in an SAM, fine tuning of the interplay between intramolecular, intermolecular, and interfacial interactions is required. Such a complete miscibility can be achieved by designing molecular components with similar chemical structures, thereby exhib-

iting energetically comparable hetero- and homomolecular interactions within the SAM. To accomplish this goal, we designed and synthesized molecule **1** and combined it with commercial undecanethiol (**2**). Both molecules bear a sulfur-

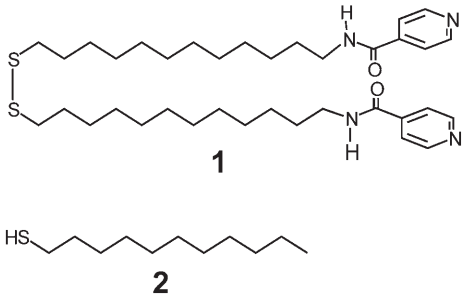

containing end group to promote covalent binding to the Au surfaces, and an alkyl backbone to favor the lateral packing within the SAMs through van der Waals interactions—also of a heteromolecular type. Moreover, molecule **1** exposes a pyridine-amide end group in the ω-position to promote directional homomolecular interactions through the formation of linear hydrogen-bonded networks.

The self-assembly of **1** and **2** in single-component SAMs was investigated by scanning tunneling microscopy (STM). The results presented herein were confirmed by performing detailed cyclic voltammetry (CV) and Fourier transform infrared reflection adsorption spectroscopy (FT-IRRAS) studies, which will be reported elsewhere.[16]

Undecanethiol (**2**) forms a densely packed SAM on Au(111). This monolayer shows a commensurate ($\sqrt{3}\times\sqrt{3}$)R30° hexagonal lattice with respect to the gold surface (see Figure 1b). We also observed the typical c($4\sqrt{3}\times 2\sqrt{3}$)R30° [or c($4\times2$)] superstructures of this hexagonal lattice. The nearest neighbors in the ($\sqrt{3}\times\sqrt{3}$)R30° structures are 0.5 nm apart. Moreover, all molecules in the lattice exhibit the same contrast in the STM images. Previous work revealed four levels of brightness associated with the c(4×2) structure. This variation in the image contrast was ascribed to the different orientations adopted by the upper methyl groups.[17,18] Conversely, molecule **1** does not form single-component, densely packed SAMs. CV, FT-IRRAS, and STM measurements provided evidence of the formation of a covalent bond between **1** and Au. However, the energetic unbalance between the different intermolecular interactions prevents the formation of long-range crystalline domains (see the Supporting Information). In fact, the interactions involved in the formation of the SAM of **1** are: 1) covalent binding between Au and the SH group, which favors the formation of a commensurate ($\sqrt{3}\times\sqrt{3}$)R30° molecular lattice with a binding-site distance of 0.5 nm; 2) van der Waals interactions among the alkyl chains, which are optimized when the chains adopt an all-*trans* conformation with a lateral interchain distance of 0.4 nm; 3) hydrogen bonding between the amide units, which is optimized when the N–O distance in the amino N–H···O=C hydrogen bond is 0.28 nm;[19] 4) π–π interactions of the pyridine moiety, which are optimal for a distance between aromatic rings of about 0.33 nm. Small variations in the optimal distances and angles for each specific interaction lead to a change in the total energy of the system. The unbalanced interactions in SAMs of **1** prevent the formation of an ordered assembly as revealed by CV measurements. The high density of defects in the SAM, together with the high insulating barrier originated by the long chain of **1**, hinders a good imaging resolution by STM (Figure 1a).

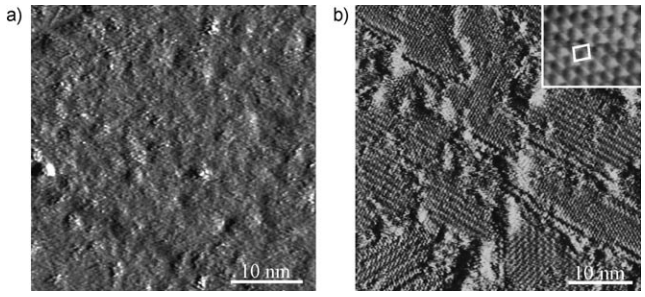

Figure 1. a) Monocomponent SAM of **1**; average tunneling current, I_t = 20 pA; bias voltage, V = 1 V. b) Monocomponent SAM of **2**; I_t = 15 pA, V = 750 mV. Inset: SAM of **2**, unit cell ($\sqrt{3}\times\sqrt{3}$)R30°.

We attempted to improve the order in the SAMs containing molecule **1** by means of co-deposition with **2**. We prepared different chemisorbed monolayers by incubating the gold substrates in solutions containing different molar ratios of molecules **1** and **2**, namely, 1/9, 3/7, 1/1, 7/3, and 9/1. The STM images recorded on monolayers obtained from solutions containing 9/1 and 7/3 ratios of the two compounds exhibited a complete and selective coverage of the monolayers with molecules of **1**, which formed poorly ordered, ultrathin films. At (**1**/**2**) molar ratios of 1/1 and 3/7, small, phase-segregated domains of **2** (marked with white arrows in Figure 2) were observed, while the monolayer was mainly covered by disordered domains of **1** (see Figure 2).

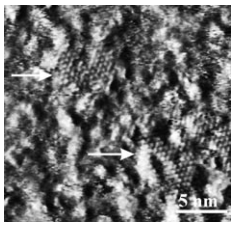

Figure 2. Mixed SAM prepared by immersion in a solution containing a 1/1 molar ratio of **1**/**2**. The white arrows show phase-segregated domains of undecanethiol; I_t = 2.8 pA; V = 867 mV.

These results are consistent with the definition of chemisorbed SAMs, which are considered to be kinetically trapped at local thermodynamic minima. The free energy of the minimum depends on the relative coverage of the phase-segregated domains. Furthermore, during SAM formation, the coverage ratio is mostly under kinetic control. Considering the case of an assembly process under complete thermodynamic control, and assuming a scenario characterized by non-miscibility between the two components, the SAMs formed will show only one phase of the molecule generating the more energetically stable assembly. In view of the Bragg–Williams model for an ideal solution, and according to its application to bicomponent SAMs, this case is reflected by two non-interacting molecules, and

therefore, by a positive and high-interaction parameter.[13] We observed that the films prepared by incubating the Au(111) substrate (for one month) in all the above-mentioned mixed solutions were fully and uniquely covered with **1** (see the Supporting Information). Therefore, although the monolayer of **1** is not densely packed, it is more thermodynamically stable than the mono-component monolayer of **2**.

Interestingly, the monolayers obtained from solutions containing compounds **1** and **2** at a molar ratio of 1/9 displayed peculiar striped domains, the relative coverage within the SAM depending on the incubation time (after two days of immersion, these SAMs exhibited striped domains). The unit cell shown in Figure 3 a,b contains two molecules:

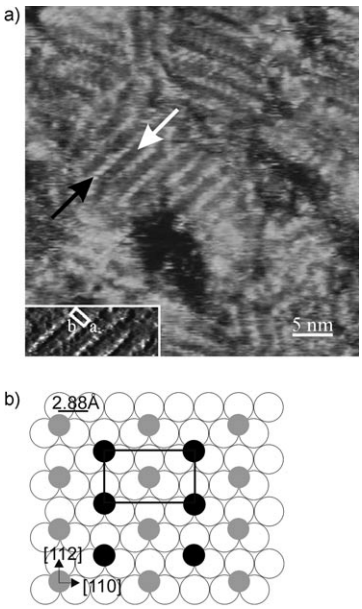

Figure 3. STM height contrast image of an SAM formed after two days of incubation in a solution containing a 1/9 molar ratio of **1/2**. Inset: unit-cell parameters: $a = (0.53 \pm 0.1)$ nm; $b = (1.2 \pm 0.1)$ nm; $\alpha = 84°$, area: 0.6 nm^2. These lattice parameters possibly indicate a commensurate lattice with a unit cell equal to $(2\sqrt{3} \times \sqrt{3})$, the gold lattice parameter being 2.88 Å. The black arrow shows a row of molecules **1**; the white arrow indicates a row of undecanethiol molecules ($I_t = 10$ pA, $V = 750$ mV). b) Sketch of the molecular packing in the bicomponent domain. The black circles represent the pyridine-amide derivatives (molecule **1**) whereas the grey circles show the undecanethiol molecules (molecule **2**).

larger and brighter spots are located at the edges of the unit cell, whereas a dark spot is found at its centre. Similar domains are typically found in monocomponent SAMs formed by alkanethiol species exposing a head group which is capable of forming hydrogen bonds, as in the cases of 1-mercaptoundecanoic acid,[20] mercaptopropionic acid,[21] and 1-mercapto-2-propanol[22] (the authors explained these structures in terms of alternating rows of hydrogen-bonded and non-H-bonded molecules).

Since it was never possible to observe ordered monocomponent SAMs of molecule **1**, we can rule out that the bidimensional structures shown in Figure 3 are formed by ordered linear arrays of **1** only. Furthermore, although it was possible to detect a darker molecular row in the striped domains, the imaging resolution turned out to be very poor, which indicates either that the molecules in this row are not as conducting as those aligned in the brightest row, and/or that this darker row contains much shorter molecules. Based on these considerations, we can conclude that the darker row is composed of an ordered alignment of **2**, a conclusion that is further supported by FT-IRRAS measurements, which provide evidence of the presence of both molecules on the Au(111) surface (see the Supporting Information).

After five days of incubation, the striped domains appeared as shown in Figure 4. The unit-cell parameters

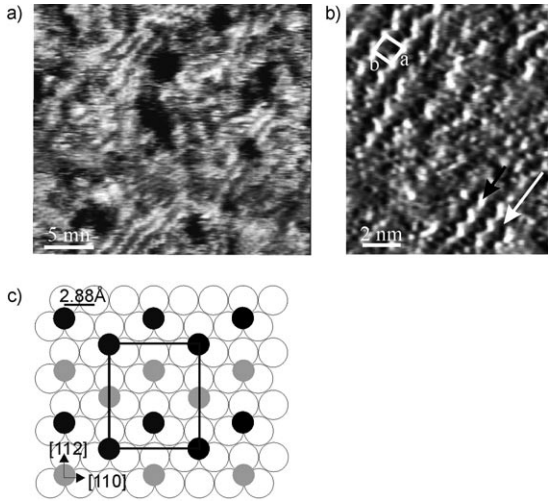

Figure 4. SAM formed after five days of incubation in a solution containing a 1/9 molar ratio of **1/2**. a) STM height contrast image; b) STM current contrast image; unit-cell parameters: $a = (1.1 \pm 0.1)$ nm; $b = (1.0 \pm 0.1)$ nm; $\alpha = 92°$, area: 1.1 nm^2 ($I_t = 2.172$ pA, $V = 810$ mV). c) Sketch of the molecular packing in the bicomponent domain.

(see Figure 4 b) are similar to the c(4 × 2) lattice parameters found for alkanethiol SAMs, which indicates that the covalent interaction between Au and S promotes an assembly commensurate with the Au(111) lattice. The appearance of a zigzag molecular array (see the black arrow in Figure 4 b) is in accordance with the structure observed in monocomponent SAMs formed by molecules containing amide moieties placed within the molecular chain.[23] FTIR studies performed by Clegg and co-workers provided evidence of the existence of intermolecular H bonds in SAMs containing amide units along the molecular chain.[24] The two molecular patterns shown in Figures 3 and 4 can be found in mixed SAMs formed from 1/9 (**1/2**) solutions, although the striped pattern presented in Figure 4 was most commonly observed. Figure 4 c depicts the proposed molecular packing in the striped domains of Figure 4 b. In this architecture, the sulfur head groups bind at a threefold hollow site of Au(111), as typically reported in the literature.[5a]

The two molecular lattices do not seem to differ in terms of binding sites, although according to the model presented in Figures 3 b and 4 c, the pyridine-amide derivative aligns along

two different directions of the Au(111) surface, namely, [112] and [110]. Therefore, the differences between the two structures might arise from distinct interchain interactions, which stabilize the molecular patterning. In fact, in the structure shown in Figure 3, the pyridine amides align exactly along a line, whereas Figure 4 exhibits the characteristic zigzag pattern. Since the structure found in Figure 4 is the most commonly observed one, we assume that the zigzag patterning adopted by molecule **1** along a row might stabilize better the H-bond interactions than the linear patterning (a molecular model that describes the zigzag patterning is reported in the Supporting Information).

To the best of our knowledge, this is the first example of the formation of SAMs composed of completely miscible bicomponent domains chemisorbed on a metallic surface. The pyridine-amide rows (represented by a black arrow in Figure 3a) are separated by thinner rows of undecanethiol (white arrow in Figure 3a), which allows the pyridine-amide unit to emerge vertically from the overall SAM. The undecanethiol row laterally stabilizes the row of **1** through van der Waals interchain interactions.

Since the striped domains were only observed at a (**1**/**2**) molar ratio of 1/9—and considering that for long incubation times the SAM is mainly formed by domains of molecule **1**—it is possible to conclude that the striped domains are formed under kinetic control (see the Supporting Information). In particular, the diffusion rate of the two molecules on the surface and the dynamic adsorption–desorption processes that lead to the final assembly are notably affected by the relative concentration of the two compounds in solution, and by their molecular structure. Kinetic control during the formation of mixed crystalline domains is also demonstrated by the observation of a high pyridine-amide coverage on the samples that were incubated (for over a month) in the 1/9 (**1**/**2**) solutions. Our results demonstrate that it is possible to trap the system in a local thermodynamic minimum containing striped domains by kinetically controlling the self-assembly process and, in particular, by varying the concentration of the two molecules in solution as well as the incubation time.

Previous studies have shown that in bicomponent SAMs obtained from solutions containing both decanethiol and an alkyl-amide derivative, the former molecules form crystalline domains whereas the latter ones preferentially align along linear decanethiol domain boundaries. This packing of the alkyl-amide derivatives has been interpreted in terms of an optimization of linear intermolecular hydrogen bonds between the amide units.[23a] However, this bicomponent system is not able to develop into a fully 2D crystalline intermixed domain, because the H bonds are buried in the SAM and the heteromolecular interactions are not favored as a consequence of the different chain composition.[23a] Such imbalance in the inner SAM heteromolecular interactions confines the two components into separated domains. Conversely, in our system, we did observe bicomponent crystalline domains. The main growth direction of the striped domains—which are only a few nanometers wide, perhaps because of their metastable nature—was found to lie on the main stripe axis, thus indicating that the major contribution to the total energy arises from intermolecular interactions among molecules aligned along the rows. The high directionality of the assembly and the detected nearest-neighbor distance of 5 Å between molecules **1** in a row indicate that the observed stabilization arises from the formation of H bonds between the amide units. In view of the confinement of molecules **1** along the rows, the pyridine functional groups are exposed outside the SAM, so that it is easier to address them. Moreover, at this position, the pyridine groups do not experience the steric constrains present in the densely packed underlayer; therefore, they can be used as specific coordination sites (for example, for the coordination of Zn porphyrins). Experiments are underway in our laboratories to achieve further stabilization of the heteromolecular interactions, aiming at a thermodynamically driven formation of crystalline mixed SAMs.

In summary, by applying a supramolecular approach to the development of chemisorbed bicomponent SAMs on Au(111), we showed—for the first time—that it is possible to form multicomponent crystalline domains in SAMs, thereby achieving subnanometer control over the molecular patterning of a surface. This represents the first, yet fundamental, step towards the controlled spatial confinement of individual molecules or functional groups on a surface. This supramolecular multicomponent array allows potential recognition of target functional groups and could therefore lead to the detection of single-molecule properties.

Experimental Section

The synthesis of **1** as well as ther experimental procedures are given in the Supporting Information.

Received: October 12, 2007
Published online: February 19, 2008

Keywords: molecular electronics · nanotechnology · scanning probe microscopy · self-assembly · supramolecular chemistry

[1] J. Huskens, M. A. Deij, D. N. Reinhoudt, *Angew. Chem.* **2002**, *114*, 4647; *Angew. Chem. Int. Ed.* **2002**, *41*, 4467.
[2] For reviews see: a) V. Balzani, A. Credi, F. M. Raymo, J. F. Stoddart, *Angew. Chem.* **2000**, *112*, 3484; *Angew. Chem. Int. Ed.* **2000**, *39*, 3348; b) W. R. Browne, B. L. Feringa, *Nat. Nanotechnol.* **2006**, *1*, 25; c) E. R. Kay, D. A. Leigh, F. Zerbetto, *Angew. Chem.* **2007**, *119*, 72; *Angew. Chem. Int. Ed.* **2007**, *46*, 72.
[3] S. S. Jang, Y. H. Jang, Y. H. Kim, W. A. Goddard, A. H. Flood, B. W. Laursen, H. R. Tseng, J. F. Stoddart, J. O. Jeppesen, J. W. Choi, D. W. Steuerman, E. Delonno, J. R. Heath, *J. Am. Chem. Soc.* **2005**, *127*, 1563.
[4] G. Pace, V. Ferri, C. Grave, M. Elbing, C. von Hänisch, M. Zharnikov, M. Mayor, M. A. Rampi, P. Samorì, *Proc. Natl. Acad. Sci. USA* **2007**, *104*, 9937.
[5] For reviews see: a) J. C. Love, L. A. Estroff, J. K. Kriebel, R. G. Nuzzo, G. M. Whitesides, *Chem. Rev.* **2005**, *105*, 1103; b) F. Schreiber, *Prog. Surf. Sci.* **2000**, *65*, 151; c) R. K. Smith, P. A. Lewis, P. S. Weiss, *Prog. Surf. Sci.* **2004**, *75*, 1.
[6] G. H. Yang, Y. L. Qian, C. Engtrakul, L. R. Sita, G. Y. Liu, *J. Phys. Chem. B* **2000**, *104*, 9059.
[7] A. A. Dameron, J. W. Ciszek, J. M. Tour, P. S. Weiss, *J. Phys. Chem. B* **2004**, *108*, 16761.

[8] B. Lussem, L. Muller-Meskamp, S. Karthauser, R. Waser, M. Homberger, U. Simon, *Langmuir* **2006**, *22*, 3021.
[9] D. Hobara, T. Kakiuchi, *Electrochem. Commun.* **2001**, *3*, 154.
[10] D. Hobara, T. Sasaki, S.-I. Imabayashi, T. Kakiuchi, *Langmuir* **1999**, *15*, 5073.
[11] R. C. Chambers, C. E. Inman, J. E. Hutchison, *Langmuir* **2005**, *21*, 4615.
[12] C. D. Bain, G. M. Whitesides, *J. Am. Chem. Soc.* **1988**, *110*, 6560.
[13] J. P. Folkers, P. E. Laibinis, G. M. Whitesides, J. Deutch, *J. Phys. Chem.* **1994**, *98*, 563.
[14] L. Y. Li, S. F. Chen, S. Y. Jiang, *Langmuir* **2003**, *19*, 3266.
[15] J.-M. Lehn, *Science* **2002**, *295*, 2400.
[16] G. Pace et al. unpublished results.
[17] A. Riposan, G. Y. Liu, *J. Phys. Chem. B* **2006**, *110*, 23926.
[18] G. E. Poirier, M. J. Tarlov, *Langmuir* **1994**, *10*, 2853.
[19] S.-W. Tam-Chang, H. A. Biebuyck, G. M. Whitesides, N. Jeon, R. G. Nuzzo, *Langmuir* **1995**, *11*, 4371.
[20] a) C. B. Gorman, Y. F. He, R. L. Carroll, *Langmuir* **2001**, *17*, 5324; b) O. Azzaroni, M. E. Vela, H. Martin, A. H. Creus, G. Andreasen, R. C. Salvarezza, *Langmuir* **2001**, *17*, 6647; c) M. L. Carot, V. A. Macagno, P. Paredes-Olivera, E. M. Patrito, *J. Phys. Chem. C* **2007**, *111*, 4294.
[21] a) M. J. Giz, B. Duong, N. J. Tao, *J. Electroanal. Chem.* **1999**, *465*, 72; b) D. Hobara, S. Imabayashi, T. Kakiuchi, *Nano Lett.* **2002**, *2*, 1021; c) S. Imabayashi, M. Iida, D. Hobara, Z. Q. Feng, K. Niki, T. Kakiuchi, *J. Electroanal. Chem.* **1997**, *428*, 33.
[22] C. K. Rhee, Y. N. Kim, *Appl. Surf. Sci.* **2004**, *228*, 313.
[23] a) P. A. Lewis, R. K. Smith, K. F. Kelly, L. A. Bumm, S. M. Reed, R. S. Clegg, J. D. Gunderson, J. E. Hutchison, P. S. Weiss, *J. Phys. Chem. B* **2001**, *105*, 10630; b) R. K. Smith, S. M. Reed, P. A. Lewis, J. D. Monnell, R. S. Clegg, K. F. Kelly, L. A. Bumm, J. E. Hutchison, P. S. Weiss, *J. Phys. Chem. B* **2001**, *105*, 1119.
[24] a) R. S. Clegg, S. M. Reed, J. E. Hutchison, *J. Am. Chem. Soc.* **1998**, *120*, 2486; b) R. S. Clegg, S. M. Reed, R. K. Smith, B. L. Barron, J. A. Rear, J. E. Hutchison, *Langmuir* **1999**, *15*, 8876.

